Sciencexpress Reports

Cell types in the mouse cortex and hippocampus revealed by single-cell RNA-seq

Amit Zeisel,[1]* Ana B. Muñoz Manchado,[1]* Simone Codeluppi,[1] Peter Lönnerberg,[1] Gioele La Manno,[1] Anna Juréus,[1] Sueli Marques,[1] Hermany Munguba,[1] Liqun He,[2] Christer Betsholtz,[2,3] Charlotte Rolny,[4] Gonçalo Castelo-Branco,[1] Jens Hjerling-Leffler,[1†] Sten Linnarsson[1†]

[1]Division of Molecular Neurobiology, Department of Medical Biochemistry and Biophysics, Karolinska Institutet, S-171 77 Stockholm, Sweden. [2]Department of Immunology, Genetics and Pathology, Rudbeck Laboratory, Uppsala University, Dag Hammarskjölds väg 20, S-751 85 Uppsala, Sweden. [3]Division of Vascular Biology, Department of Medical Biochemistry and Biophysics, Karolinska Institutet, S-171 77 Stockholm, Sweden. [4]Department of Oncology-Pathology, Karolinska Institutet, S-171 76 Stockholm, Sweden.

*These authors contributed equally to this work.

†Corresponding author. E-mail: sten.linnarsson@ki.se (S.L.); jens.hjerling-leffler@ki.se (J.H.-L.)

The mammalian cerebral cortex supports cognitive functions such as sensorimotor integration, memory, and social behaviors. Normal brain function relies on a diverse set of differentiated cell types, including neurons, glia, and vasculature. Here, we have used large-scale single-cell RNA-seq to classify cells in the mouse somatosensory cortex and hippocampal CA1 region. We found 47 molecularly distinct subclasses, comprising all known major cell types in the cortex. We identified numerous marker genes, which allowed alignment with known cell types, morphology, and location. We found a layer I interneuron expressing *Pax6* and a distinct postmitotic oligodendrocyte subclass marked by *Itpr2*. Across the diversity of cortical cell types, transcription factors formed a complex, layered regulatory code, suggesting a mechanism for the maintenance of adult cell type identity.

The brain is built from a large number of specialized cell types, enabling highly refined electrophysiological behavior, as well as fulfilling brain nutrient needs and defense against pathogens. Functional specialization allows fine-tuning of circuit dynamics, and decoupling of support functions such as energy supply, waste removal and immune defense. Cells in the nervous system have historically been classified using location, morphology, target specificity and electrophysiological characteristics, often combined with molecular markers (*1*–*5*). Systematic in situ hybridization has revealed extensive regional heterogeneity (*6*). However, none of these properties carry enough information to result, in every case, in a definitive cell type identification (*7*). Single-cell RNA-seq has been used to classify cells in spleen (*8*), lung epithelium (*9*) and embryonic brain (*10*). However, the adult nervous system has greater complexity and more cell types, presenting a challenge both to sample preparation methods and computational analysis.

Here we have used quantitative single-cell RNA-seq (*11*) to perform a molecular census of the primary somatosensory cortex (S1) and the hippocampal CA1 region, based on 3,005 single-cell transcriptomes (Fig. 1A and fig. S1, A to C). Individual RNA molecules were counted using unique molecular identifiers (UMIs; essentially tags that identify individual molecules) (*12*) (fig. S1, D to J and S2, A to E), and confirmed by single-molecule RNA FISH (fig. S2, G to I).

We used clustering to discover molecularly distinct classes of cells. Standard hierarchical clustering resulted in fragmented clusters (fig. S4), because most genes were not informative in most pairwise comparisons, and contributed at best only noise. Biclustering can overcome this problem by simultaneously clustering genes and cells. We developed BackSPIN (see supplementary methods), a divisive biclustering method based on SPIN (*13*), which revealed nine major classes of cells: S1 and CA1 pyramidal neurons, interneurons, oligodendrocytes, astrocytes, microglia, vascular endothelial cells, mural cells (that is, pericytes and vascular smooth muscle cells) and ependymal cells (Fig. 1, A and B, and fig. S3).

The dataset allowed us to identify the most specific markers for each class, many of which are known to play a functional role in these cells (fig. S5). S1 pyramidal cells were marked by *Tbr1*, a transcription factor required for the final differentiation of cortical projection neurons; oligodendrocytes by *Hapln2*, encoding a protein required for proper formation of nodes of Ranvier; mural cells by *Acta2*, a key component of actin thin filaments; and endothelial cells by *Ly6c1* [expressed by monocytes peripherally, and endothelial cells in the brain (*14*)]. Some were novel, such as *Gm11549* (a long noncoding RNA specific to S1 pyramidal neurons), *Spink8* (a serine protease inhibitor specific to hippocampal pyramidal cells), and *Pnoc* (Prepronociceptin, here identified as an interneuron marker).

By repeating biclustering on each of the nine major classes (Fig. 1C and figs. S5 to S8), we identified a total of 47 molecularly distinct subclasses of cells. Every subclass was detected in multiple mice (fig. S1K), arguing that cell identity was preserved across these genetically outbred (CD-1) animals. Neurons contained more RNA than glia and vascular cells, and a larger number of detectable genes (Fig. 1C

and fig. S1E). Mitochondrial mRNAs were less variable, although mitochondrial tRNAs were highly specifically enriched in endothelial cells (fig. S1E).

We identified seven subclasses of S1 pyramidal cells (Fig. 2A and figs. S6A and S7), which were largely layer-specific. The superficial layers II/III and IV were represented by single populations whereas layer V showed two distinct subclasses. Layer VI and VIb were represented by single populations, but in addition we found a subclass lacking specific markers but expressing common deep-layer markers such as *Pcp4*. A distinct subclass expressed *Synpr* and *Nr4a2*, which are abundant in the adjacent claustrum, with some cells extending into S1.

We found two types of CA1 glutamatergic cells (fig. S8), plus cells derived from the adjacent CA2 (as defined by *Pcp4*) and subiculum (as defined by *Ly6g6e*). Genes highly expressed in type 2 CA1 pyramidal neurons were associated with mitochondrial function (fig. S8), which has been shown to correlate with the firing rate and length of projections in cortical neurons (*15*). Orthogonal to the two main classes, we found CA1 layer-specific markers (i.e., *Calb1* and *Nov*) as well dorsoventrally patterned genes (i.e., *Wfs1* and *Grp*) (*16*), in both of the two main types of CA1 cells. These may correspond to functional differences between layers (*17*).

We found 16 subclasses of interneurons (Fig. 2B and fig. S6, C and D), but there are likely more subclasses because we achieved only shallow sampling of *Sst* and *Pvalb*-expressing cells. In superficial layers of S1 we identified an *Htr3a* and *Pax6*-expressing interneuron subclass, confirmed by immunohistochemistry (Fig. 2C) (13.9 ±2.4% of 5HT3aEGFP cells in layer I, n = 4 animals, 636 cells analyzed). These interneurons specifically expressed *Myh8*, *Fut9*, and *Manea*. In whole-cell current clamp recordings of layer 1 neurons, subsequently stained for PAX6, these cells exhibited intrinsic electrophysiological and morphological characteristics of late-spiking neurogliaform cells (6 $PAX6^+$ out of 40 recorded cells) (Fig. 2D and fig. S6E). *Pax6* is not expressed in the ventral forebrain during development, further suggesting that neurogliaform cells are developmentally heterogeneous (*18*).

CA1 and S1 regions both contained interneurons of almost every subclass (Fig. 2B) showing that interneurons residing in functionally distinct cortical structures are transcriptionally closely related. The two exceptions were cells expressing *Vip*, *Penk*, *Calb2*, and *Crh* (which were confined to S1) and cells expressing *Lhx6*, *Reln*, and *Gabrd* [which were confined to CA1 and suggested to be MGE-derived Ivy cells and neurogliaform cells (*18*)].

Astrocytes formed two subclasses (Fig. 3A and fig. S9A), distinguished by differential expression of *Gfap* (type 1) and *Mfge8* (type 2). Immunostaining showed that type 1 astrocytes were derived from layer I, particularly from the glia limitans, a thin layer made up mostly of astrocytes that is arranged against the pia (Fig. 3B). In contrast, type 2 astrocytes were more uniformly distributed in the cortex, and were smaller and less ramified.

We identified two types of immune cells: microglia (the tissue-resident macrophages of the brain) and perivascular macrophages. Although closely related, these cell types have distinct developmental origin (*19*). Both expressed brain macrophage markers *Aif1* and *Cx3cr1*, while perivascular macrophages were distinguished by expression of *Mrc1* and *Lyve1*, characteristic of pro-angiogenic perivascular type 2 macrophages (*20*). Immunohistochemistry for the corresponding proteins confirmed that microglia ($AIF1^+$/$LYVE1^-$/$MRC1^-$) had a classical, ramified morphology and were located throughout the cortex (Fig. 3, D and E). In contrast, perivascular macrophages (AIF^+/$LYVE1^+$/$MRC1^+$) were located only along vessels and showed an ameboid morphology. They were distinct from mural and endothelial cells (fig. S10). Comparison with peritoneal macrophages confirmed their identity (fig. S9A). The correlation between brain and peripheral macrophages (0.67) was similar to that between neurons and glia (0.62), underscoring the functional divergence of this immune cell class.

Six subpopulations of oligodendrocytes were identified (Fig. 3F and fig. S9C), likely representing stages of maturation: immature (Oligo4), pre-myelinating (Oligo2), myelinating (Oligo5) and terminally differentiated post-myelination (Oligo6) oligodendrocytes. An intermediate population, Oligo3, was almost exclusively observed in somatosensory cortex and may represent a distinct cellular state specific for this tissue. The subclass Oligo1, which did not express the prototypical genes associated with oligodendrocyte precursor cells (OPCs), may represent a postmitotic cellular state, associated with the first steps of oligodendrocyte differentiation. Oligo1 cells expressed a distinct set of genes, including *Itpr2*, *Prom1*, *Gpr17*, *Tcf7l2*, *9630013A20Rik*, *Idh1*, *Cnksr3*, and *Rnf122*. Single-molecule RNA FISH confirmed that *Itpr2* and *Cnksr3* were expressed in strict subsets of cells expressing *Plp1*, a pan-oligodendrocyte marker (4.5% and 7.5% respectively) (Fig. 3G). Together, the Oligo1 – Oligo6 populations may represent sequential steps in the process of maturation from an OPC to a terminally differentiated oligodendrocyte.

Across this diverse set of cell types, we found many transcription factors with highly restricted expression patterns (Fig. 4A and supplementary methods). For example, interneurons expressed key interneuron regulators *Dlx1, Dlx2, Dlx5,* and *Arx*, and pyramidal layer II/III neurons expressed *Neurog2*, which can directly reprogram human ES cells to excitatory neurons of layer II/III phenotype with near 100% efficiency (*21*). *Lyl1* and *Spic* were specific to perivascular macrophages; *Spic* is essential for the maintenance of red pulp macrophages (*22*), suggesting it may play a similar role in brain perivascular macrophages.

Expanding this analysis to all genes, we found extensive functional specialization between cellular subclasses. Ependymal cells (multiciliated cells lining the ventricles) expressed the largest set of subclass-restricted genes,

including transcription factors *Foxj1*, *Myb*, and *Rfx2*, the master regulators of motile ciliogenesis (*23*) (*24*), and *Zmynd10*, which causes ciliopathy when mutated in humans (*25*). Nearly every structural component of cilia was also represented (Fig. 4B), including the 2+9 microtubule core and radial spokes, the dynein and kinesin motors, the filamentous shell, the basal body that anchors cilia to the cytoplasm, and two adenylate kinases (*Ak7* and *Ak8*) that generate ATP energy supporting cilia motility. Many of these structural genes are directly regulated by *Foxj1, Rfx2* or *Rfx3* (*23*, *26*) (Fig. 4B).

In summary, our findings reveal the diversity of brain cell types and transcriptomes. Across the full set of cell types, transcription factors formed a complex, layered regulatory code, suggesting a plausible mechanism for the maintenance of adult differentiated cell types. More broadly, these results showcase the power of explorative single-cell RNA-seq, and point the way toward future whole-brain and even whole-organism cell type discovery and characterization. Such data will deepen our understanding of the regulatory basis of cellular identity, in development, neurodegenerative disease, and regenerative medicine.

REFERENCES AND NOTES

1. B. J. Molyneaux, P. Arlotta, J. R. Menezes, J. D. Macklis, Neuronal subtype specification in the cerebral cortex. *Nat. Rev. Neurosci.* **8**, 427–437 (2007). Medline doi:10.1038/nrn2151
2. T. Klausberger, P. Somogyi, Neuronal diversity and temporal dynamics: The unity of hippocampal circuit operations. *Science* **321**, 53–57 (2008). Medline doi:10.1126/science.1149381
3. J. DeFelipe, P. L. López-Cruz, R. Benavides-Piccione, C. Bielza, P. Larrañaga, S. Anderson, A. Burkhalter, B. Cauli, A. Fairén, D. Feldmeyer, G. Fishell, D. Fitzpatrick, T. F. Freund, G. González-Burgos, S. Hestrin, S. Hill, P. R. Hof, J. Huang, E. G. Jones, Y. Kawaguchi, Z. Kisvárday, Y. Kubota, D. A. Lewis, O. Marín, H. Markram, C. J. McBain, H. S. Meyer, H. Monyer, S. B. Nelson, K. Rockland, J. Rossier, J. L. Rubenstein, B. Rudy, M. Scanziani, G. M. Shepherd, C. C. Sherwood, J. F. Staiger, G. Tamás, A. Thomson, Y. Wang, R. Yuste, G. A. Ascoli, New insights into the classification and nomenclature of cortical GABAergic interneurons. *Nat. Rev. Neurosci.* **14**, 202–216 (2013). Medline
4. K. Sugino, C. M. Hempel, M. N. Miller, A. M. Hattox, P. Shapiro, C. Wu, Z. J. Huang, S. B. Nelson, Molecular taxonomy of major neuronal classes in the adult mouse forebrain. *Nat. Neurosci.* **9**, 99–107 (2006). Medline doi:10.1038/nn1618
5. G. Fishell, B. Rudy, Mechanisms of inhibition within the telencephalon: "Where the wild things are". *Annu. Rev. Neurosci.* **34**, 535–567 (2011). Medline doi:10.1146/annurev-neuro-061010-113717
6. E. S. Lein, M. J. Hawrylycz, N. Ao, M. Ayres, A. Bensinger, A. Bernard, A. F. Boe, M. S. Boguski, K. S. Brockway, E. J. Byrnes, L. Chen, L. Chen, T. M. Chen, M. C. Chin, J. Chong, B. E. Crook, A. Czaplinska, C. N. Dang, S. Datta, N. R. Dee, A. L. Desaki, T. Desta, E. Diep, T. A. Dolbeare, M. J. Donelan, H. W. Dong, J. G. Dougherty, B. J. Duncan, A. J. Ebbert, G. Eichele, L. K. Estin, C. Faber, B. A. Facer, R. Fields, S. R. Fischer, T. P. Fliss, C. Frensley, S. N. Gates, K. J. Glattfelder, K. R. Halverson, M. R. Hart, J. G. Hohmann, M. P. Howell, D. P. Jeung, R. A. Johnson, P. T. Karr, R. Kawal, J. M. Kidney, R. H. Knapik, C. L. Kuan, J. H. Lake, A. R. Laramee, K. D. Larsen, C. Lau, T. A. Lemon, A. J. Liang, Y. Liu, L. T. Luong, J. Michaels, J. J. Morgan, R. J. Morgan, M. T. Mortrud, N. F. Mosqueda, L. L. Ng, R. Ng, G. J. Orta, C. C. Overly, T. H. Pak, S. E. Parry, S. D. Pathak, O. C. Pearson, R. B. Puchalski, Z. L. Riley, H. R. Rockett, S. A. Rowland, J. J. Royall, M. J. Ruiz, N. R. Sarno, K. Schaffnit, N. V. Shapovalova, T. Sivisay, C. R. Slaughterbeck, S. C. Smith, K. A. Smith, B. I. Smith, A. J. Sodt, N. N. Stewart, K. R. Stumpf, S. M. Sunkin, M. Sutram, A. Tam, C. D. Teemer, C. Thaller, C. L. Thompson, L. R. Varnam, A. Visel, R. M. Whitlock, P. E. Wohnoutka, C. K. Wolkey, V. Y. Wong, M. Wood, M. B. Yaylaoglu, R. C. Young, B. L. Youngstrom, X. F. Yuan, B. Zhang, T. A. Zwingman, A. R. Jones, Genome-wide atlas of gene expression in the adult mouse brain. *Nature* **445**, 168–176 (2007). Medline doi:10.1038/nature05453
7. A. Kepecs, G. Fishell, Interneuron cell types are fit to function. *Nature* **505**, 318–326 (2014). Medline doi:10.1038/nature12983
8. D. A. Jaitin, E. Kenigsberg, H. Keren-Shaul, N. Elefant, F. Paul, I. Zaretsky, A. Mildner, N. Cohen, S. Jung, A. Tanay, I. Amit, Massively parallel single-cell RNA-seq for marker-free decomposition of tissues into cell types. *Science* **343**, 776–779 (2014). Medline
9. B. Treutlein, D. G. Brownfield, A. R. Wu, N. F. Neff, G. L. Mantalas, F. H. Espinoza, T. J. Desai, M. A. Krasnow, S. R. Quake, Reconstructing lineage hierarchies of the distal lung epithelium using single-cell RNA-seq. *Nature* **509**, 371–375 (2014). Medline doi:10.1038/nature13173
10. A. A. Pollen, T. J. Nowakowski, J. Shuga, X. Wang, A. A. Leyrat, J. H. Lui, N. Li, L. Szpankowski, B. Fowler, P. Chen, N. Ramalingam, G. Sun, M. Thu, M. Norris, R. Lebofsky, D. Toppani, D. W. Kemp 2nd, M. Wong, B. Clerkson, B. N. Jones, S. Wu, L. Knutsson, B. Alvarado, J. Wang, L. S. Weaver, A. P. May, R. C. Jones, M. A. Unger, A. R. Kriegstein, J. A. West, Low-coverage single-cell mRNA sequencing reveals cellular heterogeneity and activated signaling pathways in developing cerebral cortex. *Nat. Biotechnol.* **32**, 1053–1058 (2014). Medline doi:10.1038/nbt.2967
11. S. Islam, A. Zeisel, S. Joost, G. La Manno, P. Zajac, M. Kasper, P. Lönnerberg, S. Linnarsson, Quantitative single-cell RNA-seq with unique molecular identifiers. *Nat. Methods* **11**, 163–166 (2014). Medline doi:10.1038/nmeth.2772
12. T. Kivioja, A. Vähärautio, K. Karlsson, M. Bonke, M. Enge, S. Linnarsson, J. Taipale, Counting absolute numbers of molecules using unique molecular identifiers. *Nat. Methods* **9**, 72–74 (2011). Medline doi:10.1038/nmeth.1778
13. D. Tsafrir, I. Tsafrir, L. Ein-Dor, O. Zuk, D. A. Notterman, E. Domany, Sorting points into neighborhoods (SPIN): Data analysis and visualization by ordering distance matrices. *Bioinformatics* **21**, 2301–2308 (2005). Medline doi:10.1093/bioinformatics/bti329
14. C. Shi, E. G. Pamer, Monocyte recruitment during infection and inflammation. *Nat. Rev. Immunol.* **11**, 762–774 (2011). Medline doi:10.1038/nri3070
15. O. Kann, C. Huchzermeyer, R. Kovács, S. Wirtz, M. Schuelke, Gamma oscillations in the hippocampus require high complex I gene expression and strong functional performance of mitochondria. *Brain* **134**, 345–358 (2011). Medline doi:10.1093/brain/awq333
16. H. W. Dong, L. W. Swanson, L. Chen, M. S. Fanselow, A. W. Toga, Genomic-anatomic evidence for distinct functional domains in hippocampal field CA1. *Proc. Natl. Acad. Sci. U.S.A.* **106**, 11794–11799 (2009). Medline doi:10.1073/pnas.0812608106
17. K. Mizuseki, K. Diba, E. Pastalkova, G. Buzsáki, Hippocampal CA1 pyramidal cells form functionally distinct sublayers. *Nat. Neurosci.* **14**, 1174–1181 (2011). Medline doi:10.1038/nn.2894
18. L. Tricoire, K. A. Pelkey, M. I. Daw, V. H. Sousa, G. Miyoshi, B. Jeffries, B. Cauli, G. Fishell, C. J. McBain, Common origins of hippocampal Ivy and nitric oxide synthase expressing neurogliaform cells. *J. Neurosci.* **30**, 2165–2176 (2010). Medline doi:10.1523/JNEUROSCI.5123-09.2010
19. M. Prinz, J. Priller, Microglia and brain macrophages in the molecular age: From origin to neuropsychiatric disease. *Nat. Rev. Neurosci.* **15**, 300–312 (2014). Medline doi:10.1038/nrn3722
20. I. Galea, K. Palin, T. A. Newman, N. Van Rooijen, V. H. Perry, D. Boche, Mannose receptor expression specifically reveals perivascular macrophages in normal, injured, and diseased mouse brain. *Glia* **49**, 375–384 (2005). Medline doi:10.1002/glia.20124
21. Y. Zhang, C. Pak, Y. Han, H. Ahlenius, Z. Zhang, S. Chanda, S. Marro, C. Patzke, C. Acuna, J. Covy, W. Xu, N. Yang, T. Danko, L. Chen, M. Wernig, T. C. Südhof, Rapid single-step induction of functional neurons from human pluripotent stem cells. *Neuron* **78**, 785–798 (2013). Medline doi:10.1016/j.neuron.2013.05.029
22. M. Kohyama, W. Ise, B. T. Edelson, P. R. Wilker, K. Hildner, C. Mejia, W. A. Frazier, T. L. Murphy, K. M. Murphy, Role for Spi-C in the development of red pulp macrophages and splenic iron homeostasis. *Nature* **457**, 318–321 (2009). Medline doi:10.1038/nature07472
23. J. Thomas, L. Morlé, F. Soulavie, A. Laurençon, S. Sagnol, B. Durand, Transcriptional control of genes involved in ciliogenesis: A first step in making cilia. *Biol. Cell* **102**, 499–513 (2010). Medline doi:10.1042/BC20100035
24. E. R. Brooks, J. B. Wallingford, Multiciliated cells. *Curr. Biol.* **24**, R973–R982 (2014). Medline doi:10.1016/j.cub.2014.08.047
25. M. A. Zariwala, H. Y. Gee, M. Kurkowiak, D. A. Al-Mutairi, M. W. Leigh, T. W. Hurd, R. Hjeij, S. D. Dell, M. Chaki, G. W. Dougherty, M. Adan, P. C. Spear, J. Esteve-

Rudd, N. T. Loges, M. Rosenfeld, K. A. Diaz, H. Olbrich, W. E. Wolf, E. Sheridan, T. F. Batten, J. Halbritter, J. D. Porath, S. Kohl, S. Lovric, D. Y. Hwang, J. E. Pittman, K. A. Burns, T. W. Ferkol, S. D. Sagel, K. N. Olivier, L. C. Morgan, C. Werner, J. Raidt, P. Pennekamp, Z. Sun, W. Zhou, R. Airik, S. Natarajan, S. J. Allen, I. Amirav, D. Wieczorek, K. Landwehr, K. Nielsen, N. Schwerk, J. Sertic, G. Köhler, J. Washburn, S. Levy, S. Fan, C. Koerner-Rettberg, S. Amselem, D. S. Williams, B. J. Mitchell, I. A. Drummond, E. A. Otto, H. Omran, M. R. Knowles, F. Hildebrandt, ZMYND10 is mutated in primary ciliary dyskinesia and interacts with LRRC6. *Am. J. Hum. Genet.* **93**, 336–345 (2013). Medline

26. M. I. Chung, T. Kwon, F. Tu, E. R. Brooks, R. Gupta, M. Meyer, J. C. Baker, E. M. Marcotte, J. B. Wallingford, Coordinated genomic control of ciliogenesis and cell movement by RFX2. *eLife* **3**, e01439 (2014). Medline doi:10.7554/eLife.01439
27. S. Lee, J. Hjerling-Leffler, E. Zagha, G. Fishell, B. Rudy, The largest group of superficial neocortical GABAergic interneurons expresses ionotropic serotonin receptors. *J. Neurosci.* **30**, 16796–16808 (2010). Medline doi:10.1523/JNEUROSCI.1869-10.2010
28. A. Edelstein, N. Amodaj, K. Hoover, R. Vale, N. Stuurman, Computer control of microscopes using μManager. *Curr. Protoc. Mol. Biol.* **92**, 14.20.1–14.20.17 (2010). Medline doi:10.1002/0471142727.mb1420s92
29. A. Lyubimova, S. Itzkovitz, J. P. Junker, Z. P. Fan, X. Wu, A. van Oudenaarden, Single-molecule mRNA detection and counting in mammalian tissue. *Nat. Protoc.* **8**, 1743–1758 (2013). Medline doi:10.1038/nprot.2013.109
30. A. Raj, P. van den Bogaard, S. A. Rifkin, A. van Oudenaarden, S. Tyagi, Imaging individual mRNA molecules using multiple singly labeled probes. *Nat. Methods* **5**, 877–879 (2008). Medline doi:10.1038/nmeth.1253
31. A. B. Muñoz-Manchado, C. Foldi, S. Szydlowski, L. Sjulson, M. Farries, C. Wilson, G. Silberberg, J. Hjerling-Leffler, Novel striatal GABAergic interneuron populations labeled in the 5HT3aEGFP mouse. *Cereb. Cortex* (2014). Medline doi:10.1093/cercor/bhu179
32. D. Tsafrir, I. Tsafrir, L. Ein-Dor, O. Zuk, D. A. Notterman, E. Domany, Sorting points into neighborhoods (SPIN): Data analysis and visualization by ordering distance matrices. *Bioinformatics* **21**, 2301–2308 (2005). Medline doi:10.1093/bioinformatics/bti329
33. G. Getz, E. Levine, E. Domany, Coupled two-way clustering analysis of gene microarray data. *Proc. Natl. Acad. Sci. U.S.A.* **97**, 12079–12084 (2000). Medline doi:10.1073/pnas.210134797
34. E. Levine, E. Domany, Resampling method for unsupervised estimation of cluster validity. *Neural Comput.* **13**, 2573–2593 (2001). Medline doi:10.1162/089976601753196030
35. B. J. Frey, D. Dueck, Clustering by passing messages between data points. *Science* **315**, 972–976 (2007). Medline doi:10.1126/science.1136800
36. R. Cangelosi, A. Goriely, Component retention in principal component analysis with application to cDNA microarray data. *Biol. Direct* **2**, 2 (2007). Medline doi:10.1186/1745-6150-2-2

ACKNOWLEDGMENTS

The raw data has been deposited with the Gene Expression Omnibus (www.ncbi.nlm.nih.gov/geo) under accession code GSE60361. Annotated data are available at http://linnarssonlab.org/cortex. We thank P. Ernfors, K. Harris, and R. Sandberg for useful comments on the manuscript; F. Ginhoux for helpful discussions on microglia and macrophages; A. Johnsson for laboratory management and support; ALM/SciLife (H. G. Blom) for technical support; and Fluidigm Inc. (R.C. Jones and M. Lynch) for generous technical and instrument support. S.L. was supported by the European Research Council (261063, BRAINCELL) and the Swedish Research Council (STARGET); A.Z. was supported by the Human Frontier Science Program; A.M.-M. was supported by Karolinska Institutet (BRECT); C.R. was supported by the Swedish Cancer Society (CAN2013/852); G.C.-B. was supported by Swedish Research Council, European Union (FP7/Marie Curie Integration Grant EPIOPC), Åke Wiberg foundation, Karolinska Institutet Research Foundations, Svenska Läkaresällskapet, Clas Groschinskys Minnesfond and Hjärnfonden; J.H.-L. was supported by Swedish Research Council, European Union (FP7/Marie Curie Actions (322304, Adolescent Dev)), StratNeuro, Jeanssons- Åke Wibergs- and Magn Bergvalls Foundations. Supplementary materials contain additional data.

SUPPLEMENTARY MATERIALS

www.sciencemag.org/cgi/content/full/science.aaa1934/DC1
Materials and Methods
Supplementary Text
Figs. S1 to S11
Tables S1 and S2
References (*27*–*36*)

30 October 2014; accepted 30 January 2015
Published online 19 February 2015
10.1126/science.aaa1934

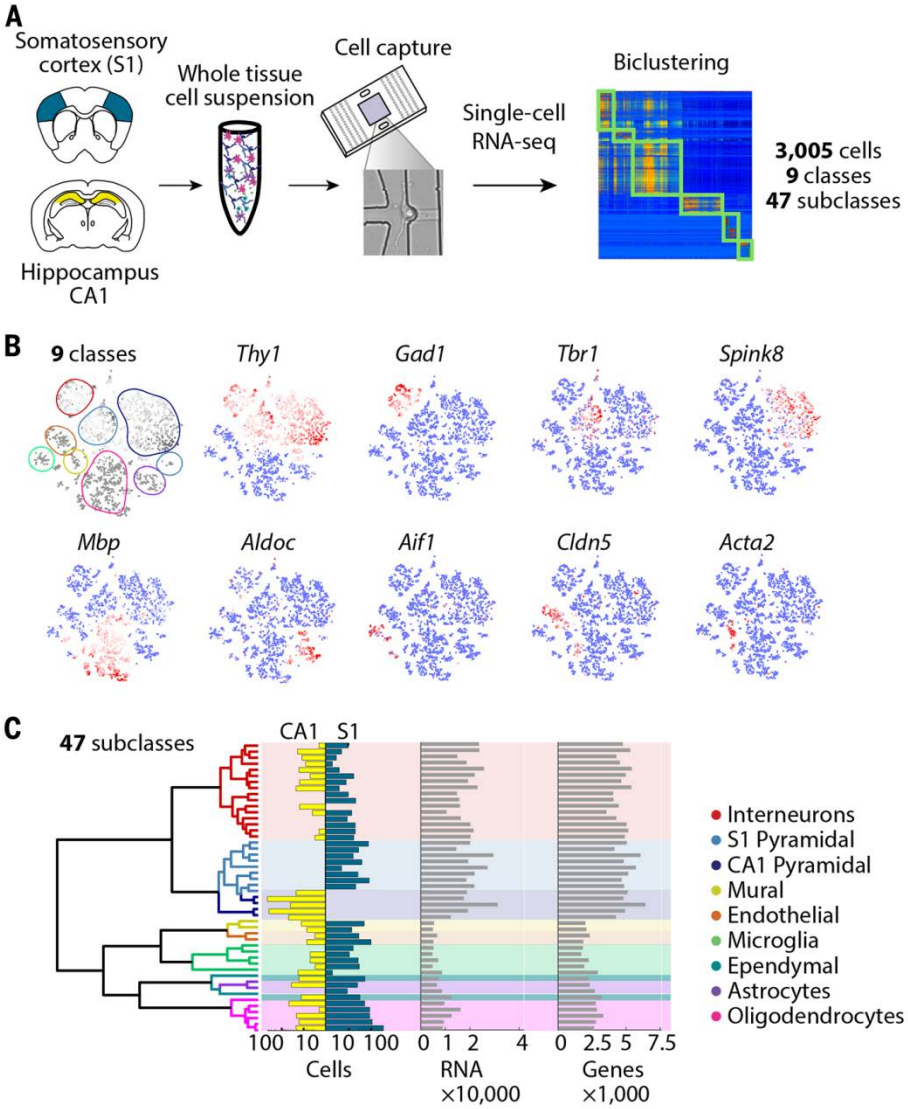

Fig. 1. Molecular census of somatosensory S1 cortex and hippocampus CA1 by unbiased sampling and single-cell RNA-seq. (**A**) Workflow for obtaining and analyzing single-cell RNA-seq from juvenile mouse cortical cells, from dissection to single-cell RNA-seq and biclustering. (**B**) Visualization of nine major classes of cells using t-Distributed Stochastic Neighbor Embedding (tSNE). Each dot is a single cell, and cells are laid out to show similarities. Colored contours correspond to the nine clusters in (A) and fig. S3. Expression of known markers is shown using the same layout (blue, no expression; white, 1% quantile; red, 99% quantile). (**C**) Hierarchical clustering analysis on 47 subclasses. Barplots show number of captured cells in CA1 and S1, number of detected polyA+ RNA molecules per cell, and total number of genes detected per cell.

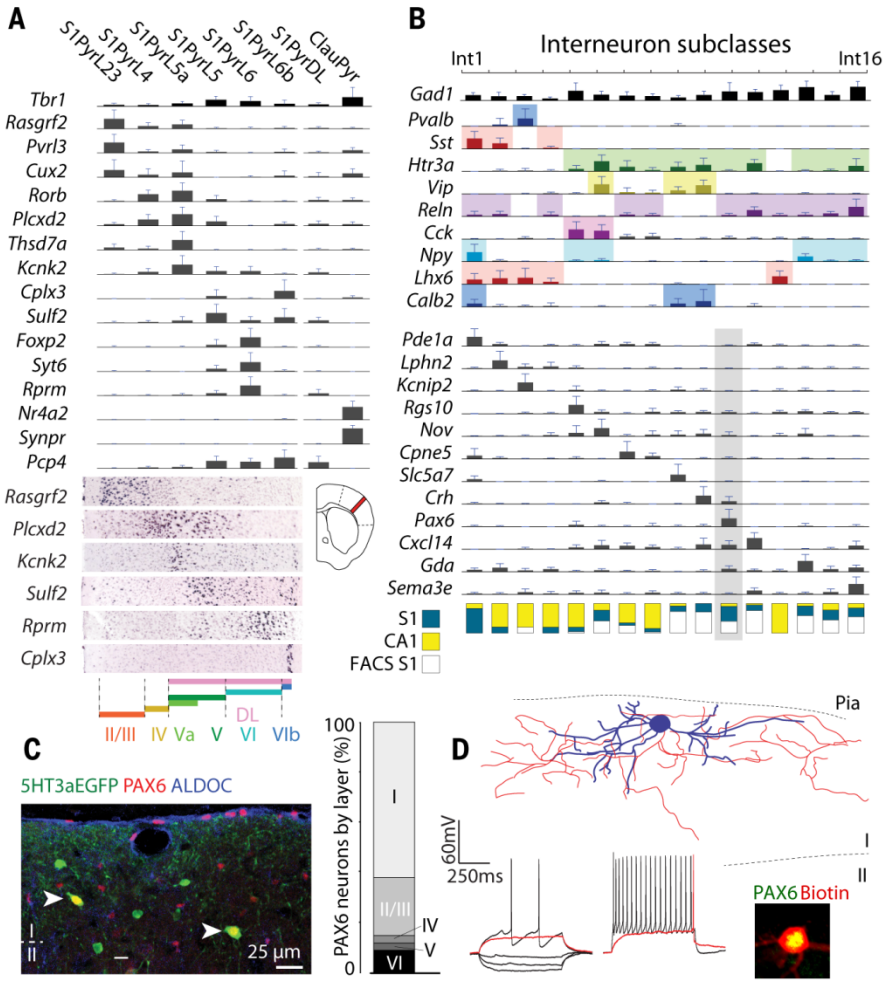

Fig. 2. Neuron subclasses in the somatosensory cortex. (**A**) Subclasses of pyramidal neurons in the somatosensory cortex (S1) identified by BackSPIN clustering. Barplots show mean expression of selected known and novel markers (error bars show standard deviations). Layer-specific expression shown by in situ hybridization (Allen Brain Atlas). S1PyrL23, layer II-III; S1PyrL4, layer IV; S1PyrL5a, layer Va; S1PyrL5, layer V; S1PyrL6, layer VI; S1PyrL6b, layer VIb; S1PyrDL, deep layers; ClauPyr, claustrum. (**B**) Identification of interneuron subclasses. Barplots show selected known and novel markers. Fraction of S1/CA1 cells is depicted at bottom: blue, S1; yellow, CA1; white, flow sorted Htr3a^{+} cells from S1. (**C**) Immunohistochemistry demonstrating the existence and localization of novel PAX6^{+}/5HT3aEGFP^{+} interneurons, Int11. Barplots show the layer distribution of these neurons. (**D**) Intrinsic electrophysiology and morphology of PAX6^{+} interneurons in S1 layer I, identified by post hoc staining.

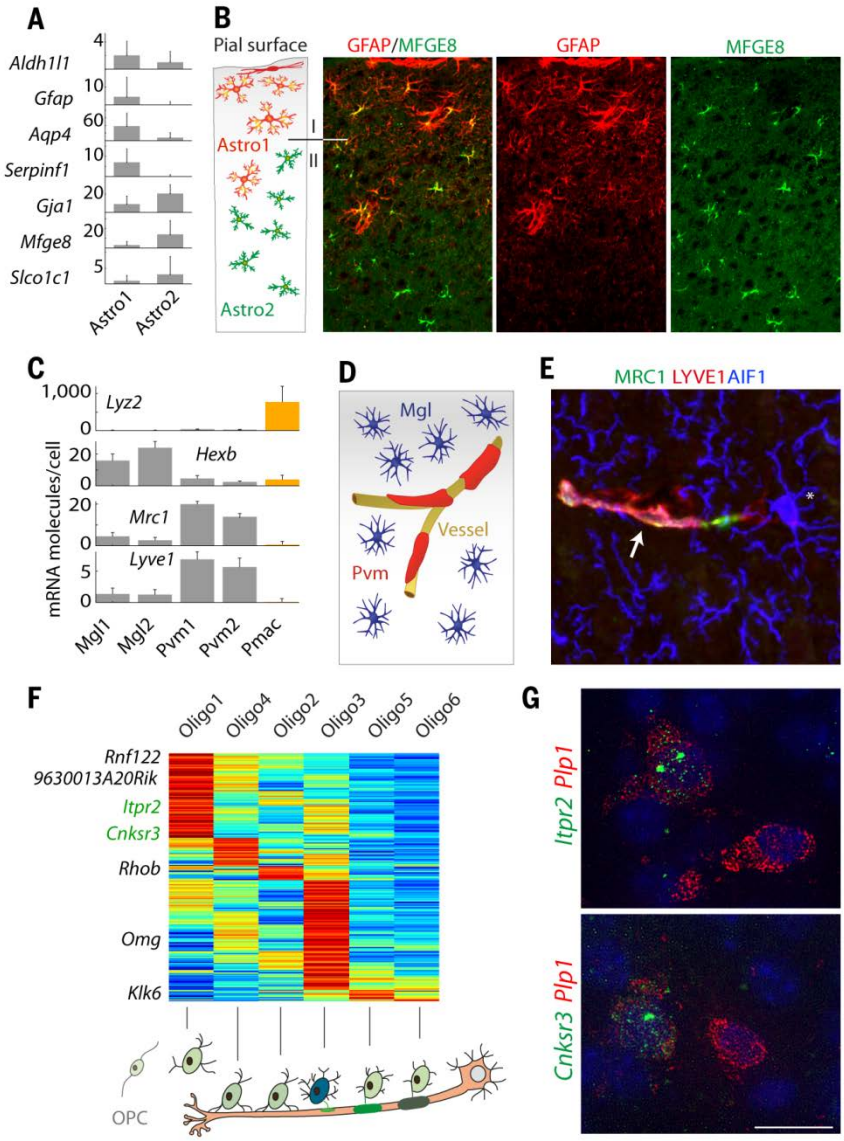

Fig. 3. Characterization of glial subclasses. Caption(**A**) Two types of astrocytes (Astro1 and Astro2) identified by common and distinct markers. (**B**) Immunohistochemistry for GFAP (red, Astro1) and MFGE8 (green, Astro2). (**C**) Genes showing expression restricted to microglia (Mgl), perivascular macrophages (Pvm) and peritoneal macrophages (Pmac). Error bars show standard deviations. (**D**) Cartoon illustrating the morphology and localization of microglia and perivascular macrophages. (**E**) Immunostaining for AIF1 (previously known as Iba-1, blue) marking microglia, and for MRC1 (green) and LYVE1 (red) marking perivascular macrophages. Asterisk, a microglia cell. Arrow, a perivascular macrophage aligned to a vessel (not stained). (**F**) Heatmap showing progressive changes in gene expression along oligodendrocyte differentiation, illustrated below. (**G**) Single-molecule RNA FISH for *Itpr2* and *Cnksr3* mark a strict subset of oligodendrocytes (as identified by *Plp1*).

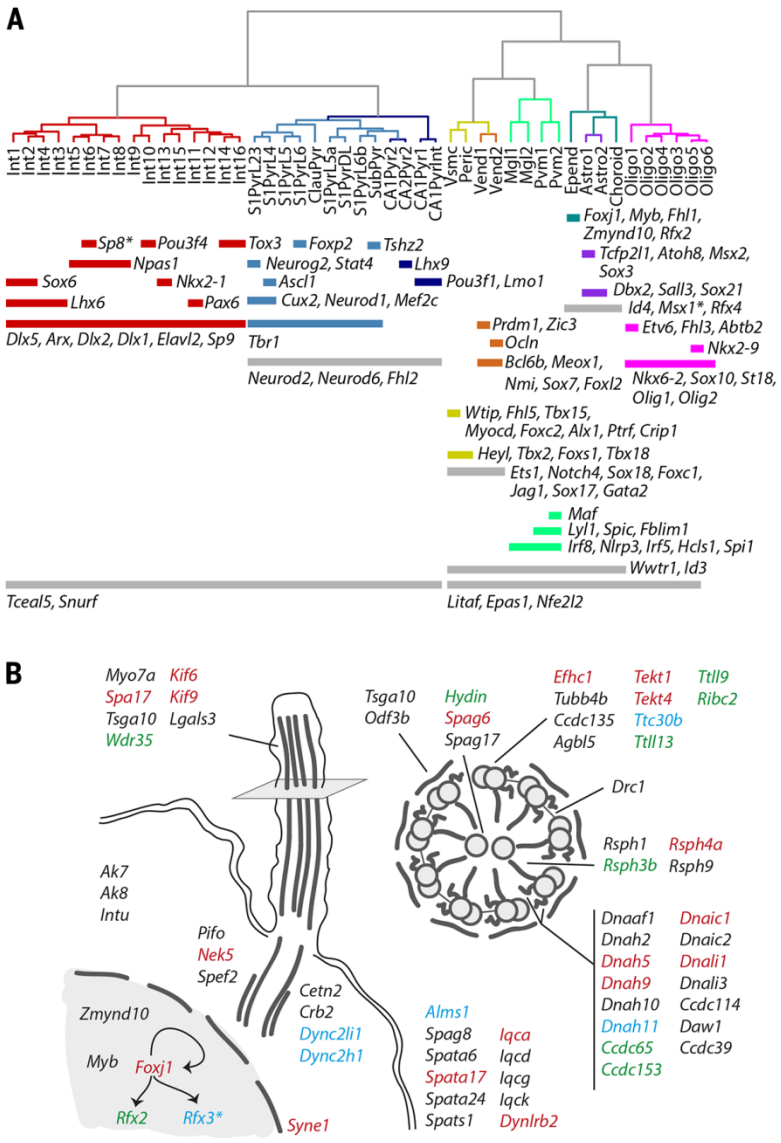

Fig. 4. Expression of regulatory genes across 47 subclasses. Caption(**A**) Transcription factors showing restricted expression across cell types. Asterisks denote genes with additional expression in distinct subclasses: *Sp8* in Int11, *Msx1* in vascular cells and microglia. (**B**) Genes specific to ependymal cells. Transcription factors *Foxj1*, *Rfx2* and *Rfx3* (with asterisk to indicate its wider expression), and their known targets are shown in red, green and blue, respectively. Arrows indicate known direct interactions between transcription factors. Only genes with known ciliary function are included.

Cell types in the mouse cortex and hippocampus revealed by single-cell RNA-seq

Amit Zeisel, Ana B. Muñoz Manchado, Simone Codeluppi, Peter Lönnerberg, Gioele La Manno, Anna Juréus, Sueli Marques, Hermany Munguba, Liqun He, Christer Betsholtz, Charlotte Rolny, Gonçalo Castelo-Branco, Jens Hjerling-Leffler and Sten Linnarsson (February 19, 2015)

published online February 19, 2015

Editor's Summary

Science (print ISSN 0036-8075; online ISSN 1095-9203) is published weekly, except the last week in December, by the American Association for the Advancement of Science, 1200 New York Avenue NW, Washington, DC 20005.